Quantification of right atrial fibrosis by cardiac magnetic resonance: verification of the method to standardize thresholds.

Cuantificación de fibrosis auricular derecha mediante resonancia magnética cardiaca:verificación del método para estandarización de umbrales.

Clara Gunturiz-Beltrán (MD)[a,b,c], Roger Borràs (MSc)[a,b,d], Francisco Alarcón (MSc)[a,b], Paz Garre (MSc)[a,b], Rosa M Figueras I Ventura (MSc, PhD)[e], Eva M Benito (MD)[a,b], Gala Caixal (MD)[a,b], Till F Althoff (MD, PhD)[a,f,g], Jose María Tolosana (MD, PhD)[a,b], Elena Arbelo (MD, PhD)[a,b], Ivo Roca (MD, PhD)[a,b], Susanna Prat-Gonzalez (MD, PhD)[a,b], Rosario Jesus Perea (MD, PhD)[a,b], Josep Brugada (MD, PhD)[a,b], Marta Sitges (MD, PhD)[a,b,c], Eduard Guasch (MD, PhD)[a,b,c], Lluís Mont (MD, PhD)[a,b,c]

The last 2 authors share senior authorship.

a.Institut Clínic Cardiovascular, Hospital Clínic, Universitat de Barcelona, Catalonia, Spain.
b.Institut d´Investigacions Biomédiques August Pi i Sunyer (IDIBAPS), Barcelona, Catalonia, Spain.
c.Centro de Investigación Biomédica en Red de Enfermedades Cardiovasculares (CIBERCV), Madrid, Spain.
d.Centro de Investigación Biomédica en Red de Salud Mental (CIBERSAM), Instituto de Salud Carlos III, Madrid, Spain.
e.ADAS3D Medical S.L., Barcelona, Catalonia, Spain
f.Department of Cardiology and Angiology, Charité-University Medicine Berlin, Charité Campus Mitte, Berlin, Germany
g.DZHK (German Centre for Cardiovascular Research), Partner Site Berlin, Berlin, Germany

Corresponding author:

Lluís Mont
Arrhythmia Section, Cardiovascular Clinic Institute, Hospital Clínic, Universitat de Barcelona.
Villarroel 170, 08036. Barcelona, Catalonia, Spain
Phone : +34-932271778
Fax : +34-934513045
E-mail : lmont@clinic.cat

CONFLICTS OF INTERESTS

Dr. Lluís Mont has received research grants, support for fellowship program, and honoraria as consultant and lecturer from Abbott; Boston Scientific; Medtronic and Biosense. Dr. Lluís Mont is a shareholder for Galgo Medical SL.

Dr. Marta Sitges has received research grants and honoraria as consultant and speaker from Abbott, Medtronic and Edwards Lifesciences.

FUNDING

This work was supported in part by a grant from the European Union Horizon 2020 Research and Innovation Programme under grant agreement [No 633196] (CATCH ME project); Instituto de Salud Carlos III [PI16/00435, PI19/00573]; Agència de Gestió d'Ajuts Universitaris i de Recerca [AGAUR, 2017 SGR 1548]; Fundació la Marató de TV3 [20152730]; CERCA Programme/Generalitat de Catalunya. The sponsor has not been involved in the study design, the data collection, the analysis or interpretation of the results, the writing of the manuscript, or the decision to publish the work.

Word count: 5000 words

ABSTRACT

Introduction and objectives: Late gadolinium-enhanced cardiac magnetic resonance (LGE-CMR) allows non-invasive detection of left atrial fibrosis in patients with atrial fibrillation (AF). However, whether the same methodology can be used in the right atrium (RA) remains unknown. Our aim was to define a standardized threshold to characterize RA fibrosis in LGE-CMR.

Methods: A 3 Tesla LGE-CMR was performed in 53 individuals; the RA was segmented and the image intensity ratio (IIR) calculated for the RA wall using 1,557,767 IIR pixels (40 994 ± 10 693 per patient). The upper limit of normality of the IIR (mean IIR + 2 standard deviation) was estimated in healthy volunteers (n = 9), and patients who had undergone previous typical atrial flutter ablation (n = 9) were used to establish the dense scar threshold. Paroxysmal and persistent AF patients (n = 10 each) were used for validation. IIR values were correlated with a high-density bipolar voltage map in 15 patients undergoing AF ablation.

Results: The upper normality limit (total fibrosis threshold) in healthy volunteers was set at an IIR = 1.21. In the post-ablation group, 60% of the maximum IIR pixel (dense fibrosis threshold) was calculated as IIR = 1.29. Endocardial bipolar voltage showed a weak but significant correlation with IIR. The overall accuracy between the electro-anatomical map and LGE-CMR to characterize fibrosis was 56%.

Conclusions: An IIR > 1.21 was determined to be the threshold for the detection of right atrial fibrosis, while an IIR > 1.29 differentiates interstitial fibrosis from dense scar. Despite differences between the left and right atria, fibrosis could be assessed with LGE-CMR using similar thresholds in both chambers.

Keywords: atrial fibrillation; right atrium; fibrosis; magnetic resonance.

RESUMEN

Introducción y objetivos: La resonancia magnética cardiaca con realce tardío de gadolinio (RMC-RTG) permite la detección no invasiva de la fibrosis auricular izquierda en pacientes con fibrilación auricular (FA). Sin embargo, se desconoce si se puede utilizar la misma metodología en la aurícula derecha (AD). Nuestro objetivo fue definir un umbral estandarizado para caracterizar la fibrosis auricular derecha mediante RMC-RTG.

Métodos: Se tomaron RMC-RTG de 3 Tesla en 53 personas; se segmentó la AD y se calculó la razón de intensidad de imagen (RII) para la pared de la AD utilizando 1.557.767 píxeles RII (40.994 ± 10.693 por paciente). El límite superior de normalidad de RII (RII promedio + 2 desviaciones estándar) se estimó en voluntarios sanos (n = 9); para establecer el umbral de cicatriz densa, se utilizaron pacientes que se habían sometido previamente a una ablación del *flutter* auricular típico (n = 9). Se incluyó a pacientes con FA paroxística y persistente (n = 10 cada grupo) para la validación. Los valores de RII se correlacionaron con un mapa de voltaje bipolar de alta densidad en 15 pacientes sometidos a ablación de FA.

Resultados: El límite superior de normalidad (umbral de fibrosis total) en voluntarios sanos se fijó en un RII = 1,21. En el grupo post-ablación, el 60% del píxel RII máximo (umbral de fibrosis densa) se calculó como RII = 1,29. El voltaje bipolar endocárdico mostró una correlación con RII débil pero significativa. La precisión general entre el mapa electro-anatómico y RMC-RTG para caracterizar la fibrosis fue del 56%.

Conclusiones: Se determinó un RII > 1,21 como umbral para la detección de fibrosis de aurícula derecha, mientras que un RII > 1,29 diferencia la fibrosis intersticial de la cicatriz densa. A

pesar de las diferencias entre las aurículas izquierda y derecha, la fibrosis pudo evaluarse con RMC-RTG usando umbrales similares en ambas cámaras.

Palabras clave: fibrilación auricular; aurícula derecha; fibrosis; resonancia magnética.

Abbreviations:

AF: atrial fibrillation

EAM: electro-anatomical map

IIR: image intensity ratio

LGE-CMR: late gadolinium-enhanced cardiac magnetic resonance

RA: right atrium

Abreviaturas:

FA: fibrilación auricular

MEA: mapa electro-anatómico

RII: ratio intensidad imagen

RMC-RTG: resonancia magnética cardiaca con realce tardío gadolinio

AD: aurícula derecha

INTRODUCTION

Atrial fibrosis is a determinant in the pathogenesis of atrial fibrillation (AF). Technical advances in recent years have enabled non-invasive characterization of atrial fibrosis by means of late gadolinium-enhanced cardiac magnetic resonance (LGE-CMR),[1] fostering numerous potential clinical applications. LGE-CMR may be useful to personalize AF ablation with both first[2] and re-do[3] procedures benefitting from previous characterization of atrial fibrosis.[4] Discontinuities (gaps) in anatomical lesions induced by ablation have shown to predict AF recurrences.[5] Finally, LGE-CMR could aid in selecting patients needing chronic anticoagulation for primary prevention of stroke.[6] However, the lack of standardized algorithms for fibrosis assessment and their variable reproducibility have limited the uptake and widespread use of LGE-CMR in clinical practice.[7]

There are anatomical, functional, and molecular differences between the left atrium (LA) and the right atrium (RA). The contribution of the RA to AF pathology remains disputed, but clinical insights underpin a central role of the RA in some patients. The RA may be particularly sensitive to damage inflicted by sleep apnea and other respiratory diseases,[8,9] and ectopic foci sustaining AF have occasionally been localized in the RA.[10] Unfortunately, our knowledge on the contribution of the RA to AF substrate is, at least in part, jeopardized by technical limitations. For example, efforts in recent years have been directed towards the non-invasive identification of atrial fibrosis in the LA, but no study has yet tested whether similar algorithms are applicable to the RA. Few small studies have employed CMR to measure fibrosis in the RA, including a case series.[11] In patients with AF and sinus node dysfunction Akoum et al. found that fibrosis burden was higher in the left than in the right atrium.[12] However, these algorithms had never been validated for RA fibrosis assessment.

Our objective was to define and validate a standardized, systematic, reproducible, and robust method to identify myocardial fibrosis in the RA by mean of LGE-CMR.

METHODS

The study protocol conforms to the Declaration of Helsinki and was approved by our institution research ethics committee (HCB/2018/0382). All patients provided signed informed consent. The data that support the findings of this study are available from the corresponding author, upon reasonable request. A comprehensive description of the methods is provided in the supplementary data.

Study design and cohorts under study

A systematic, sequential workflow[13] was used in different cohorts (figure 1) to determine RA wall intensity differentiating healthy from fibrotic tissue as well as interstitial fibrosis from dense scar. This descriptive technical study is meant to set the basics for the interpretation of fibrosis measured by LGE-CMR in RA (figure 2).

A total of 53 individuals in whom an LGE-CMR had been obtained were included in consecutive stages of this study. Initially, thresholds to identify fibrosis in the RA were determined in healthy volunteers (18 to 30-year-old individuals who had been recruited to assess LA fibrosis threshold,[13] n = 9) and patients who had undergone typical atrial flutter and AF ablation in the same procedure (n = 9, LGE-CMR performed 3 months post-ablation). Later, patients with paroxysmal (n = 10) or persistent (n = 10) AF were used for validation (LGE-CMR obtained 2 weeks before ablation procedure). Finally, correlation between the image intensity ratio (IIR) and the electroanatomical bipolar voltage map (EAM) in an additional prospective cohort of patients undergoing a first AF ablation procedure was evaluated (n = 15).

Both the RA and LA were segmented from 3 Tesla (T) LGE-CMR (Magnetom Prisma Siemens Healthcare, Germany) images with ADAS 3D software (figure 3), and 3D shells were built.

Signal intensity from each pixel of the RA wall was normalized to the mean LA blood intensity to calculate the IIR. All IIR values were represented in histograms, and the total fibrosis threshold was set as the mean IIR value in the healthy volunteers group plus 2 standard deviations (SD) which ensures that ≈ 97.5% of all pixels in the healthy volunteers group fell below this threshold. The dense scar threshold was defined as the IIR value corresponding to 60% of the maximum normalized intensity pixel in the RA of patients who had undergone cavotricuspid isthmus ablation, as previously defined in the LA.[3] Overall, healthy tissue, interstitial fibrosis, and dense scar were derived from IIR values.

Finally, in 15 consecutive patients undergoing AF ablation, bipolar voltage in an intraprocedural high density point-by-point EAM of the RA (Lasso or Pentarray catheters, CARTO 3, Biosense-Webster, USA - California) was correlated to IIR values. Only EAM points projected on the CMR shell less than 10 mm apart were used. Standard voltage thresholds of 0.1 mV and 0.5 mV were used to characterize atrial dense scar, interstitial fibrosis, and healthy tissue.

Statistical analysis

Continuous variables are shown as mean ± SD or median (interquartile range) except if otherwise stated, and groups compared with one-way ANOVA. The correlation between IIR and EAM was assessed using the Pearson correlation coefficient (r), and a generalized linear mixed model with random intercept accounted for repeated IIR measurements per patient. A 2-sided type I error of 5% was used for all tests. All analyses were performed using R v3.5.1 (R project for Statistical Computing).

RESULTS

Baseline characteristics of the population

The characteristics of the 4 study groups are shown in table 1. Most participants were males (71%). Young individuals with no risk factors were recruited for the healthy volunteer group. AF groups included middle-aged individuals with a similar burden of cardiovascular risk factors; structural heart disease was uncommon. Echocardiography was only available for AF patients and showed mild LA anteroposterior diameter enlargement (41 ± 6 mm). CMR showed a progressive enlargement of the RA from healthy volunteers to persistent AF.

Characterization of the pixel intensity in the RA

Overall, standardized LGE-CMR intensity values (i.e., IIR) of 2,283,069 pixels were obtained from both atria of all participants: 1 557 767 pixels from the RA (40 994 ± 10 693 pixels per patient), and 725 302 pixels from the LA (19 087 ± 11 414 pixels per patient). When all participants were analyzed altogether, the average IIR was higher in the LA than in the RA (IIR 0.99; 95% confidence interval [95%CI], 0.97-1.02; vs 0.77; 95%CI, 0.74-0.79; respectively; P < .0001) (table 2).

Figure 4A shows the IIR histograms for the RA; LA histograms are provided for reference. We first characterized these histograms to determine how IIR values (i.e., atrial fibrosis) were distributed on the RA. In all groups, the IIR histogram was asymmetric, with a long right tail distribution (mean skewness 0.64; a 0 value denotes a symmetrical distribution) showing that some RA areas have very dense fibrotic patches. Patients with persistent AF had the smallest

kurtosis (3.63; a kurtosis of 3 characterizes a normal distribution), revealing a larger dispersion of IIR values. Conversely, the larger kurtosis (4.66), reflecting a lower dispersion of IIR values around the mean, was observed in healthy volunteers.

Threshold determination

Normal IIR values of the RA myocardium were defined from healthy, young individuals. The upper limit of normality (mean IIR + 2SD) was calculated to be IIR = 1.21 (figure 4B). Therefore, all values with an IIR > 1.21 were considered to represent atrial fibrosis in the RA. Subsequently, the dense scar threshold was established in the group of patients who had undergone cavotricuspid isthmus ablation. As expected, in most cases the maximum intensity pixel value in the RA was located in the cavotricuspid isthmus (figure 3B, bottom panel), while other high intensity pixels located superior and inferior cava vein, appendage, septum and peri-sinus coronary ostium (figure 5). The 60% of the maximum intensity pixel was calculated as IIR = 1.29, which was therefore used to discriminate interstitial fibrosis from dense scar (figure 4B).

The interindividual reproducibility was assessed with the interobserver Lin concordance correlation coefficient in a subset of ten randomly selected right atria, segmented by 2 different independent observers. Correlation was 0.92 (0.68-0.98) for total fibrosis and 0.97 (0.89-0.99) for dense scar (table 3).

Validation of RA total fibrosis, interstitial fibrosis, and dense scar thresholds

The percentage of total, interstitial fibrosis and dense RA scar pixels were quantified in all groups to validate thresholds. The results are shown in table 4. Healthy volunteers had the lowest total RA fibrosis burden, followed by paroxysmal and persistent AF patients, and the largest amount of RA fibrosis was found in post-ablation patients. Subsequently, interstitial fibrosis and dense scar were quantified separately. Healthy volunteers and paroxysmal AF patients showed the least interstitial fibrosis, while persistent AF patients showed the greatest. Finally, post-ablation showed the largest dense scar, as expected. We found a strong association between interstitial fibrosis burden and the RA area (r = 0.84).

Correlation of EAM and CMR

A point-by-point correlation between the EAM and IIR of the RA was evaluated in 15 patients undergoing a first AF ablation procedure. Overall, 11 404 voltage values were registered, and 8 830 (407 [324-560] points per patient) remained after excluding those located > 10 mm apart from the CMR shell. A weak but significant negative correlation was found between the log-transformed bipolar voltage and the IIR (r = -0.19; $P < .0001$ in correlation analysis; beta = -1.39; 95%CI, -1.54 to -1.23; $P < .0001$ in generalized linear mixed modeling) (figure 6).

Subsequently, each of EAM- and IIR-paired points were labelled as healthy tissue, interstitial fibrosis or dense scar, and agreement between the 2 was tested (table 5). In comparison with EAM, LGE-CMR tended to underestimate RA fibrosis (healthy tissue CMR 81.0%; 95%CI, 80.2-81.8 vs EAM 60.6%; 95%CI, 59.6-61.6 for LGE-CMR and EAM, respectively). The overall agreement between the 2 techniques was 56%.

Then, bipolar voltage was averaged in each of the 3 LGE-CMR areas (e.g., healthy tissue, interstitial fibrosis, dense scar). Bipolar voltage progressively increased from LGE-CMR-

labelled areas as dense scar (mean EAM bipolar value 0.91 mV; 95%CI, 0.52-1.31) to interstitial fibrosis (1.11 mV; 95%CI, 0.72-1.50) to healthy tissue (1.77 mV; 95%CI, 1.40-2.15; *P* < .0001). Similarly, IIR progressively decreased from EAM-labelled areas as dense scar (mean IIR 0.87; 95%CI, 0.82-0.91) to interstitial fibrosis (IIR 0.81; 95%CI, 0.76-0-86) to healthy tissue (IIR 0.76; 95%CI, 0.72-0.81; *P* < .0001) (figure 7).

The left atria of the same 15 patients were used as a comparator for accuracy. In 15 479 EAM points (968 [700-1,382] points per patient), we obtained a weak but significant negative correlation between the log-transformed bipolar voltage and the IIR (r = -0.17; *P* < .0001; beta = -1.52; 95%CI, -1.62 to -1.42; *P* < .0001), similar to results in the RA.

DISCUSSION

In this study we describe a standardized method to assess RA fibrosis by means of LGE-CMR. Our results show that: *a)* an IIR > 1.21 characterizes myocardial fibrosis in the RA, while dense scar may be identified by an IIR > 1.29; and *b)* the IIR shows a weak but significant association with bipolar voltage in the RA.

LGE-CMR thresholds for atrial fibrosis are similar in the left and the right atria

Several methods have been proposed to characterize LA fibrosis.[1] The validated UTAH method[2] relies on the bimodal (healthy vs fibrosis) distribution of LA pixel intensity, but largely depends on the choice of an expert-led threshold.[14] The IIR was later designed to improve interindividual reproducibility.[15] Subsequently, characterization of healthy volunteers and patients who had undergone PV isolation enabled standardized categorization into healthy

atrial myocardium, interstitial fibrosis and dense scar.[13] We chose healthy volunteers at a very low risk of AF (i.e., aged less than 30 years) to minimize the degree of ageing-induced interstitial fibrosis, thereby establishing a fibrosis threshold beyond which AF risk increases. Following an analogous approach, in the present study we found that although IIR values characterizing fibrosis in the RA were different to those previously established for the LA, these differences were minor and, potentially, of little clinical relevance. Indeed, an IIR > 1.21 identified fibrosis in the RA, and an IIR > 1.29 differentiated interstitial fibrosis from dense scar, compared to an IIR > 1.20 and IIR > 1.32 for total fibrosis and dense scar in the LA, respectively. Structural, molecular, and functional differences between the left and right atria are evidenced by their distinct average IIR. However, despite these differences between the 2 atria,[16] fibrosis might be assessed with LGE-CMR using similar thresholds in both chambers.

Interestingly, the correlation between EAM and CMR was statistically significant but of a weak intensity, similar to findings in the LA.[17] At least partially, such a low correlation might result from technical inaccuracies and other factors accounting for a decreased correlation, such as atrial size.[17] Of note, histological assessment is the only gold standard for atrial fibrosis assessment, but its obtention is not feasible in healthy individuals. The accuracy of atrial voltage to estimate atrial fibrosis is uncertain. It is likely that structural and functional data provided by CMR and EAM, respectively, yield complementary information on the atrial remodeling. Finally, late gadolinium enhancement locates in fibrotic areas, but also may represent inflammation or portions of venous embryologic origin.

Right atrium fibrosis and remodeling in atrial fibrillation pathology

The driving role of the LA in sustaining AF in most patients is widely acknowledged. However, the RA also undergoes remarkable changes, and CMR,[12] computed tomography scan[18] and

EAM[19] data suggest a similar remodeling intensity in both atria. In some cases, however, the RA might be particularly relevant to AF pathology and therapy. Some conditions superimpose an excessive pressure and volume overload in the RA.[20] Amongst AF patients, those with obstructive sleep apnea present with decreased conduction velocity, lower electrogram voltage and a higher complexity in the RA than those without sleep apnea; notwithstanding, electrophysiological remodeling is also evident in sleep apnea patients.[9] In patients with atrial septal defects undergoing closure, RA dysfunction is a better predictor of incident AF than left atrial echocardiographic indices.[21] This may also hold true in settings such as congenital heart disease, or reentrant arrhythmias after cardiac surgery, among others.

Overall, a "right origin AF", characterized by right atrial ectopia and a right-to-left dominant frequency gradient during AF, has been claimed in some patients.[22,23] "Right AF" associates with a smaller PV, LA, and left appendage, but larger right appendage.[22] These data highlight the need for better characterization of the biatrial substrate in patients with AF. Our results will enable a more detailed, non-invasive characterization of RA fibrosis in patients with AF and, particularly, in those in which the RA could play a predominant pathophysiological role.

Clinical implications of right atrium fibrosis assessment

Myocardial fibrosis is a hallmark of AF pathology, and its characterization in the daily clinical practice may have remarkable prevention, prognostic, and therapeutic implications. LGE-CMR has arisen as a potentially powerful tool to non-invasively assess atrial fibrosis, with most efforts focused in the LA. Unfortunately, data on an optimized methodology for RA fibrosis quantification was lacking, so it remains underexplored.

The DECAAF trial proved that pre-existing LGE-CMR detected LA fibrosis predicts post-ablation outcomes,[2] but it is unknown whether characterization of RA fibrosis yields additive information. Extra-PV foci sustaining AF have been found in approximately 20% of patients with AF, and in up to 35% with permanent AF.[10] Personalized ablation protocols targeting extra-PV fibrosis in the LA have been investigated in randomized clinical trials. Both the DECAAF II[24] and ALICIA[25] trials recently failed to show improved outcomes when fibrotic patches were targeted. However, ablation of non-PV foci arising from the superior and inferior vena cava, the crista terminalis, the foramen ovale and the coronary sinus ostium[10] has shown to terminate AF in some patients. Dedicated studies are needed to determine whether targeting LGE-CMR detected RA fibrotic patches will serve to personalize ablation procedures. Finally, the role of LA fibrosis estimation to flag those individuals at high risk of incident AF is still speculative, although supported by small studies.[26] If confirmed, patients with potentially "right AF" may benefit from RA fibrosis estimation. Testing for these potential applications warrant a dedicated, optimized, and refined methodology to quantify RA fibrosis; our findings are crucial for that purpose.

Limitations

Some limitations of our work should be acknowledged. Although blood pool normalization aims at compensating inter-individual variability, other parameters may still account for significant variability in correlation analyses. Interelectrode distance, catheter disposition and mapping density might not be completely comparable amongst groups and could modify the results. Technical inaccuracies should not be disregarded. Registration errors in the EAM due to pressure on the atrial wall, or cardiac and respiratory movements may yield subtle changes in catheter position that could have a large impact on correlation analyses. Correlation analyses were performed in a point-by-point basis in 3D shells; alternative flattening

methods[27] or reducing the EAM-to-CMR tolerance distance (i.e., 10 mm in our study) may yield more accurate correlations.[17]

External reproducibility of our thresholds is critical to ensure wide clinical application of RA fibrosis assessment. We used a 3.0T CMR setup that yields a high signal-to-noise ratio and enables improved image resolution. LA thresholds previously derived from 3.0T images[13] have been recently validated in 1.5T setups;[28] whether RA thresholds may be applied in 1.5T CMR setups needs to be proved. Similarly, images were obtained 20 minutes after gadolinium administration to reach enough image contrast;[29] shorter delays may result in different thresholds. Finally, our RA thresholds have been obtained under specific parameters (see methods in the supplementary data) commonly used for LA fibrosis assessment, enabling the use of a single sequence for LA and RA fibrosis assessment; validity under different parameters cannot be ensured. We have recently shown good intra- and inter-observer reproducibility even in the hands of non-experienced operators.[30]

CONCLUSIONS

The IIR threshold of the RA to determine healthy/fibrotic tissue was established at 1.21, close to the value used for the LA. Fibrosis quantification with CMR-LGE is feasible, and could be useful, in both atria.

WHAT IS KNOWN ABOUT THE TOPIC?

- Atrial fibrosis is a determinant in the pathogenesis of AF as part of the structural remodeling.
- LGE-CMR allows non-invasive characterization of atrial fibrosis, and it could personalize AF ablation.
- Research have been focused in determining fibrosis in the LA, but no study has yet done about right atrial fibrosis assessment in magnetic resonance. This limits our ability to comprehensively characterize its contribution to AF pathology.

WHAT DOES THIS STUDY ADD?

- Thresholds identifying right atrial fibrosis in LGE-CMR: the IIR values above 1.21 identify total atrial fibrosis (interstitial fibrosis and dense scar-if present), and IIR above 1.29 discern dense scar from interstitial fibrosis.
- IIR values to localize myocardial fibrosis are similar in the LA and RA.
- Endocardial bipolar voltage correlates with IIR in the RA.

FUNDING

This work was supported in part by a grant from the European Union Horizon 2020 Research and Innovation Programme under grant agreement [No 633196] (CATCH ME project); Instituto de Salud Carlos III [PI16/00435, PI19/00573]; Agència de Gestió d'Ajuts Universitaris i de Recerca [AGAUR, 2017 SGR 1548]; Fundació la Marató de TV3 [20152730]; CERCA Programme/Generalitat de Catalunya. The sponsor has not been involved in the study design, the data collection, the analysis or interpretation of the results, the writing of the manuscript, or the decision to publish the work.

AUTHORS' CONTRIBUTION

C. Gunturiz-Beltrán: conceptualization, methodology, validation, formal analysis, investigation, resources, data curation, original draft writing, review writing and editing, visualization. R. Borràs: methodology, software, formal analysis. F. Alarcón, P. Garre, R. M. Figueras i Ventura: methodology, software. E.M Benito: conceptualization, methodology. G. Caixal, T. F, Althoff, J. M. Tolosana, E. Arbelo, I. Roca, J. Brugada: conceptualization, visualization. S. Prat-Gonzalez, R. J. Perea: software, visualization. M. Sitges: conceptualization, visualization, validation. E. Guasch: conceptualization, methodology, validation, formal analysis, investigation, resources, review writing and editing, visualization, supervision. L. Mont: conceptualization, methodology, validation, resources, review writing and editing, supervision, project administration, funding acquisition.

CONFLICTS OF INTERESTS

L. Mont has received research grants, support for fellowship program, and honoraria as consultant and lecturer from Abbott, Boston Scientific, Medtronic, and Biosense; and is a shareholder for Galgo Medical S.L. M. Sitges has received research grants and honoraria as consultant and speaker from Abbott, Medtronic, and Edwards Lifesciences. The remaining authors declare no conflicts of interest.

APPENDIX. SUPPLEMENTARY DATA

Supplementary data associated with this article can be found in the online version available at

REFERENCES

1. Oakes RS, Badger TJ, Kholmovski EG, et al. Detection and quantification of left atrial structural remodeling with delayed-enhancement magnetic resonance imaging in patients with atrial fibrillation. *Circulation*. 2009;119:1758-1767.

2. Marrouche NF, Wilber D, Hindricks G, et al. Association of atrial tissue fibrosis identified by delayed enhancement MRI and atrial fibrillation catheter ablation: the DECAAF study. *JAMA*. 2014;311:498-506.

3. Bisbal F, Guiu E, Cabanas-Grandío P, et al. CMR-guided approach to localize and ablate gaps in repeat AF ablation procedure. *JACC Cardiovasc Imaging*. 2014;7:653-663.

4. Segerson NM, Daccarett M, Badger TJ, et al. Magnetic resonance imaging-confirmed ablative debulking of the left atrial posterior wall and septum for treatment of persistent atrial fibrillation: rationale and initial experience. *J Cardiovasc Electrophysiol*. 2010;21:126-132.

5. Linhart M, Alarcon F, Borràs R, et al. Delayed Gadolinium Enhancement Magnetic Resonance Imaging Detected Anatomic Gap Length in Wide Circumferential Pulmonary Vein Ablation Lesions Is Associated With Recurrence of Atrial Fibrillation. *Circ Arrhythm Electrophysiol*. 2018;11:e006659.

6. Daccarett M, Badger TJ, Akoum N, et al. Association of left atrial fibrosis detected by delayed-enhancement magnetic resonance imaging and the risk of stroke in patients with atrial fibrillation. *J Am Coll Cardiol*. 2011;57:831-838.

7. Longobardo L, Todaro MC, Zito C, et al. Role of imaging in assessment of atrial fibrosis in patients with atrial fibrillation: State-of-the-art review. *Eur Heart J Cardiovasc Imaging*. 2014;15:1-5.

8. Caglar IM, Dasli T, Caglar FNT, Teber MK, Ugurlucan M, Ozmen G. Evaluation of atrial conduction features with tissue doppler imaging in patients with chronic obstructive pulmonary disease. *Clin Res Cardiol*. 2012;101:599-606.

9. Dimitri H, Ng M, Brooks AG, et al. Atrial remodeling in obstructive sleep apnea: implications for atrial fibrillation. *Heart Rhythm*. 2012;9:321-327.

10. Calkins H, Kuck KH, Cappato R, et al. 2012 HRS/EHRA/ECAS Expert Consensus Statement on Catheter and Surgical Ablation of Atrial Fibrillation: Recommendations for Patient Selection, Procedural Techniques, Patient Management and Follow-up, Definitions, Endpoints, and Research Trial Design. *Heart Rhythm*. 2012;9:632-696.e21.

11. Sato T, Tsujino I, Ohira H, et al. Right atrial late gadolinium enhancement on cardiac magnetic resonance imaging in pulmonary hypertension. *Circ J*. 2012;76:238-239.

12. Akoum N, McGann C, Vergara G, et al. Atrial fibrosis quantified using late gadolinium enhancement MRI is associated with sinus node dysfunction requiring pacemaker implant. *J Cardiovasc Electrophysiol*. 2012;23:44-50.

13. Benito EM, Carlosena-Remirez A, Guasch E, et al. Left atrial fibrosis quantification by late gadolinium-enhanced magnetic resonance: a new method to standardize the thresholds for reproducibility. *Europace*. 2017;19:1272-1279.

14. McGann CJ, Kholmovski EG, Oakes RS, et al. New Magnetic Resonance Imaging-Based Method for Defining the Extent of Left Atrial Wall Injury After the Ablation of Atrial Fibrillation. *J Am Coll Cardiol*. 2008;52:1263-1271.

15. Khurram IM, Beinart R, Zipunnikov V, et al. Magnetic resonance image intensity ratio, a normalized measure to enable interpatient comparability of left atrial fibrosis. *Heart Rhythm*. 2014;11:85-92.

16. Smorodinova N, Lantová L, Bláha M, et al. Bioptic Study of Left and Right Atrial Interstitium in Cardiac Patients with and without Atrial Fibrillation: Interatrial but Not Rhythm-Based Differences. *PLoS One*. 2015;10:e0129124.

17. Caixal G, Alarcón F, Althoff TF, et al. Accuracy of left atrial fibrosis detection with cardiac magnetic resonance: correlation of late gadolinium enhancement with endocardial voltage and conduction velocity. *Europace*. 2021;23:380-388.

18. Akutsu Y, Kaneko K, Kodama Y, et al. Association between left and right atrial remodeling with atrial fibrillation recurrence after pulmonary vein catheter ablation in patients with paroxysmal atrial fibrillation a pilot study. *Circ Cardiovasc Imaging* 2011;4:524-531.

19. Prabhu S, Voskoboinik A, McLellan AJA, et al. A comparison of the electrophysiologic and electroanatomic characteristics between the right and left atrium in persistent atrial fibrillation: Is the right atrium a window into the left? *J Cardiovasc Electrophysiol*. 2017;28:1109-1116.

20. Houck CA, Lanters EAH, Heida A, et al. Distribution of Conduction Disorders in Patients With Congenital Heart Disease and Right Atrial Volume Overload. *J Am Coll Cardiol EP* 2020;6:537–548.

21. Vitarelli A, Mangieri E, Gaudio C, Tanzilli G, Miraldi F, Capotosto L. Right atrial function by speckle tracking echocardiography in atrial septal defect: Prediction of atrial fibrillation. *Clin Cardiol*. 2018;41:1341-1347.

22. Hasebe H, Yoshida K, Iida M, et al. Differences in the structural characteristics and distribution of epicardial adipose tissue between left and right atrial fibrillation. *Europace*. 2018;20:435-442.

23. Hasebe H, Yoshida K, Iida M, Hatano N, Muramatsu T, Aonuma K. Right-to-left frequency gradient during atrial fibrillation initiated by right atrial ectopies and its augmentation by adenosine triphosphate: Implications of right atrial fibrillation. *Heart Rhythm*. 2016;13:354-363.

24. Marrouche NF, Wazni OM, Greene T, et al. DECAAF II: efficacy of DE-MRI-guided fibrosis ablation vs. conventional catheter ablation of persistent atrial fibrillation. In: *ESC Congress*.; August, 2021. https://esc365.escardio.org/presentation/238817?_ga=2.81001623.1615516082.1655647275-444216582.1639827571

25. Bisbal F, Benito E, Teis A, et al. Magnetic Resonance Imaging-Guided Fibrosis Ablation for the Treatment of Atrial Fibrillation: The ALICIA Trial. *Circ Arrhythm Electrophysiol*. 2020;13:e008707.

26. Peritz DC, Catino AB, Csecs I, et al. High-intensity endurance training is associated with left atrial fibrosis. *Am Heart J*. 2020;226:206-213.

27. Nunez-Garcia M, Bernardino G, Alarcon F, Caixal G, Mont L, Camara CB O. Fast Quasi-Conformal Regional Flattening of the Left Atrium. *IEEE Trans Vis Comput Graph.* 2020;26:2591-2602.

28. Bertelsen L, Alarcón F, Andreasen L, et al. Verification of threshold for image intensity ratio analyses of late gadolinium enhancement magnetic resonance imaging of left atrial fibrosis in 1.5T scans. *Int J Cardiovasc Imaging*. 2020;36:513-520.

29. Chubb H, Aziz S, Karim R, et al. Optimization of late gadolinium enhancement cardiovascular magnetic resonance imaging of post-ablation atrial scar: a cross-over study. *J Cardiovasc Magn Reson*. 2018;20:30.

30. Mrgulescu AD, Nuñez-Garcia M, Alarcón F, et al. Reproducibility and accuracy of late gadolinium enhancement cardiac magnetic resonance measurements for the detection of left atrial fibrosis in patients undergoing atrial fibrillation ablation procedures. *Europace*. 2019;21:724-731.

FIGURES AND FIGURE LEGENDS

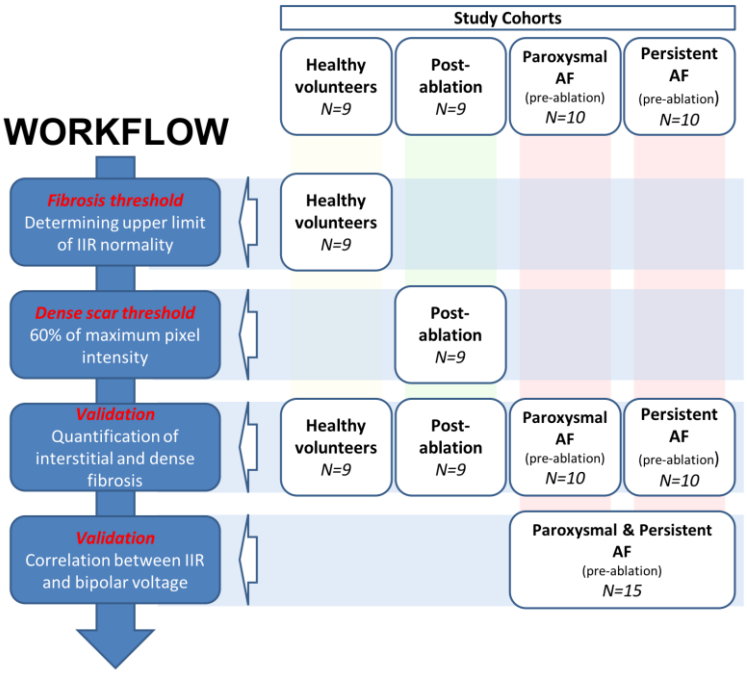

Figure 1. Workflow, cohorts used in the present study and summary of the workflow. AF, atrial fibrillation; IIR, image intensity ratio.

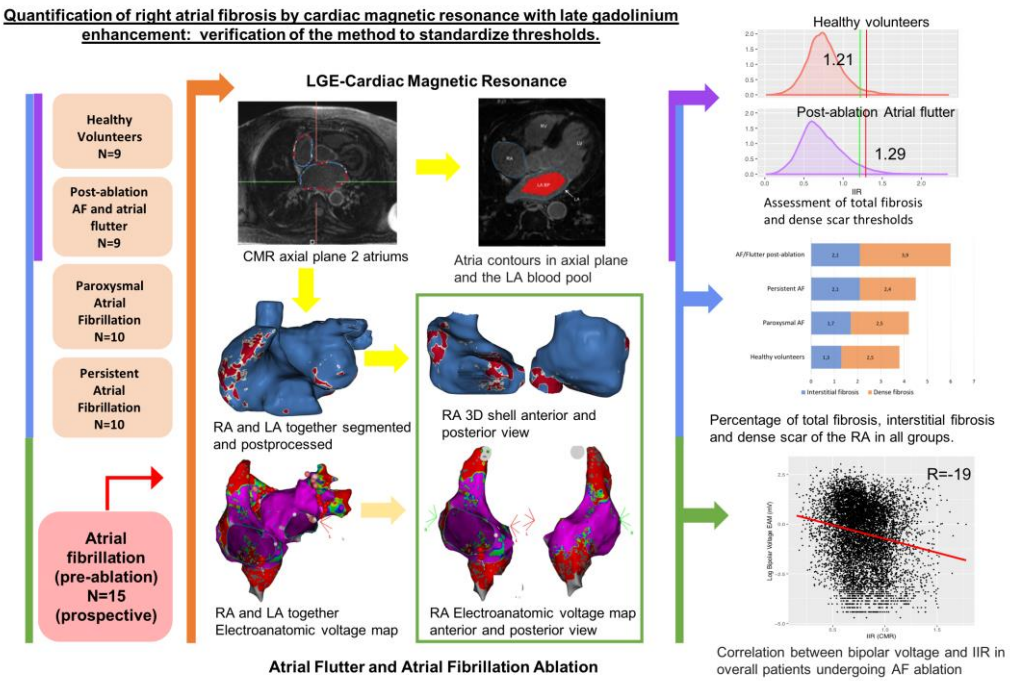

Figure 2. Central illustration. Quantification of right atrial fibrosis by cardiac magnetic resonance with late gadolinium enhancement. A: assessment of RA total fibrosis and dense scar thresholds in healthy volunteers and patients with typical atrial flutter and AF ablation in the same procedure, respectively. Application of the obtained thresholds to paroxysmal and persistent AF groups of patients. B: correlation between LGE-CMR and electro-anatomical map in a prospective group of patients undergoing AF ablation. AF, atrial fibrillation; CMR, cardiac magnetic resonance; IIR, image intensity ratio; LA, left atrium; LGE, late gadolinium enhancement; RA, right atrium.

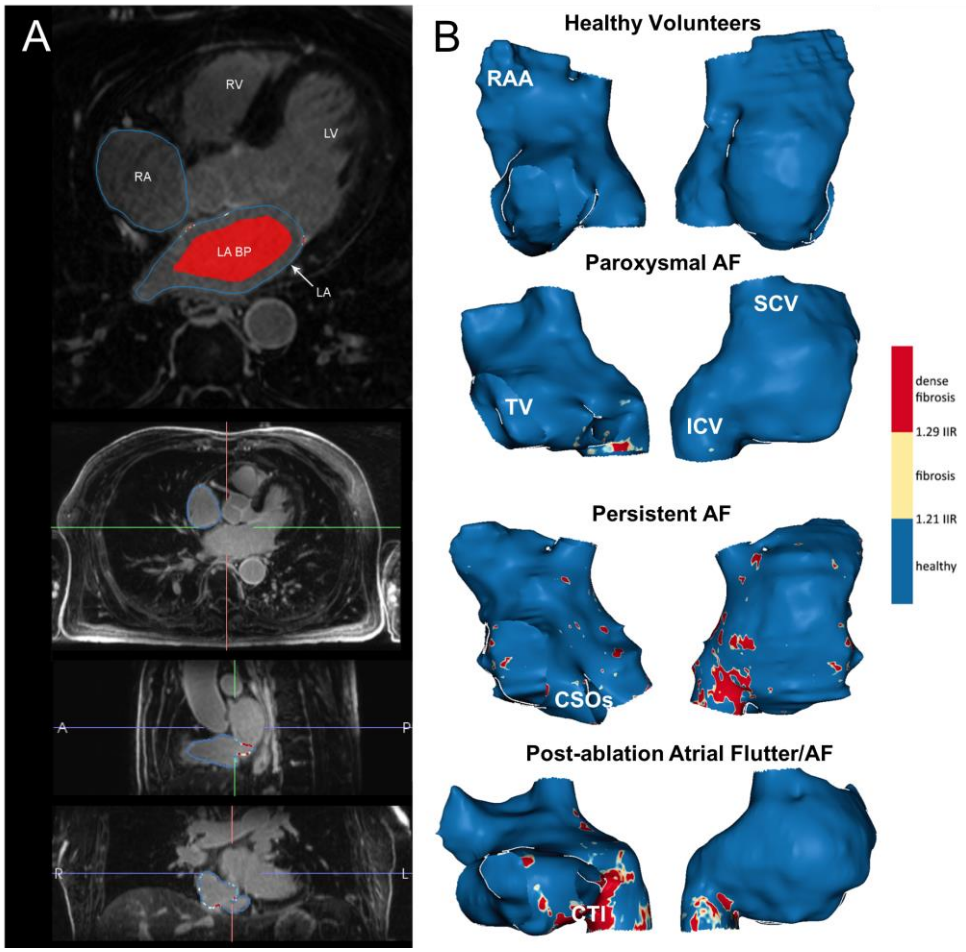

Figure 3. A: postprocessing of LGE-CMR images. In the upper panel, the RA and LA contours have been drawn manually in an axial plane; the LA blood pool is shown in red. The 3 lower panels show axial, sagittal and coronal planes of a CMR during RA segmentation. B: anteroseptal (right) and posterolateral (left) views of representative examples of RA in all the study groups. AF, atrial fibrillation; BP, blood pool; CSOs, coronary sinus ostium; CTI, cavo-tricuspid isthmus; ICV, inferior cava vein; LA, left atrium; LV, left ventricle; RA, right atrium; RAA, right atrium appendage; RV, right ventricle; SCV, superior cava vein; TV, tricuspid valve.

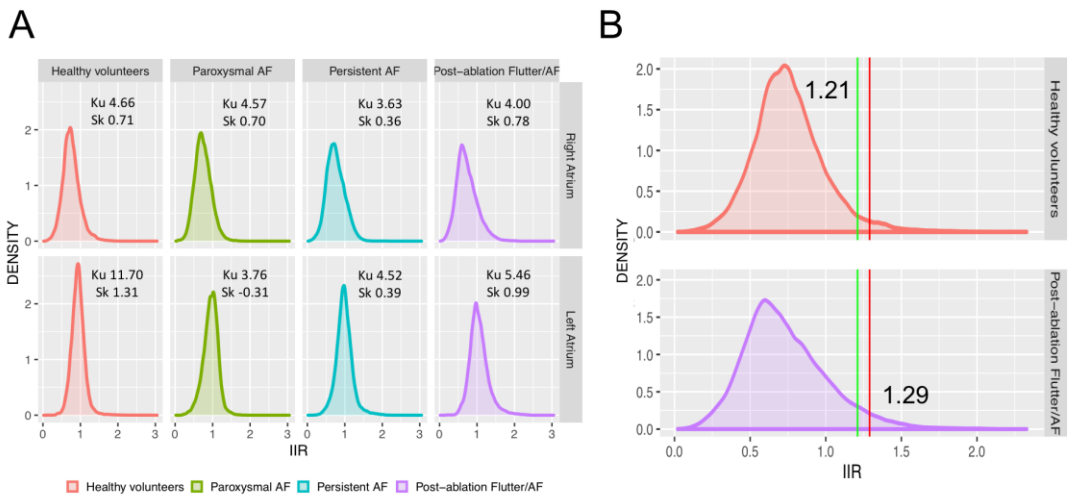

Figure 4. A: density distribution of IIR values for the RA and LA in all subgroups. B: identification of thresholds for healthy myocardial tissue (green line, measured in healthy population) and dense scar (red line, measured in previously ablated patients) over RA histograms of all subgroups. AF, atrial fibrillation; IIR, image intensity ratio; Ku, kurtosis; Sk, skewness.

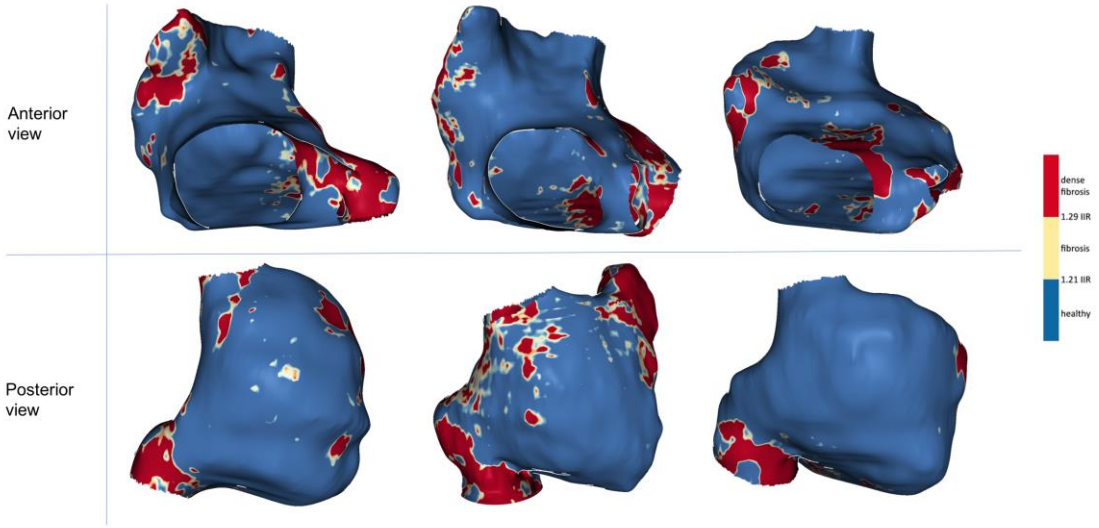

Figure 5. Examples of 3 CMR-LGE shells, depicting common high signal intensity areas in red. IIR, image intensity ratio.

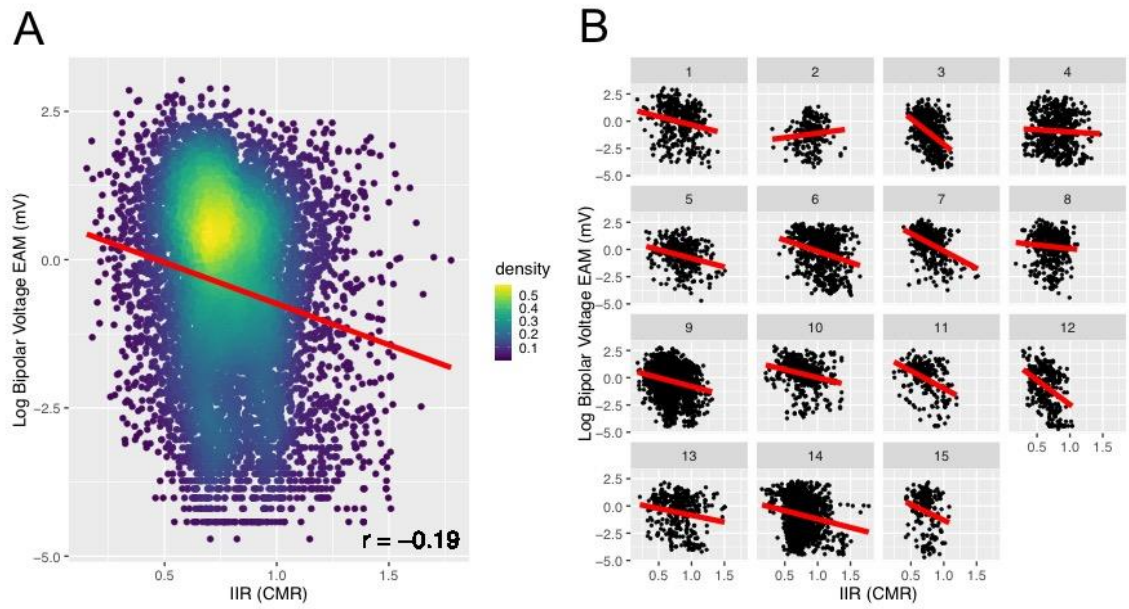

Figure 6. Correlation between bipolar voltage and IIR in the 15 patients undergoing AF ablation. A: overall correlation in the pooled cohort. Rather than a simple linear regression, analysis was performed with a generalized linear mixed model with random intercept to account for repeated IIR measurements per patient. B: analysis at the patient level. CMR, cardiac magnetic resonance; EAM, electro-anatomical map; IIR, image intensity ratio.

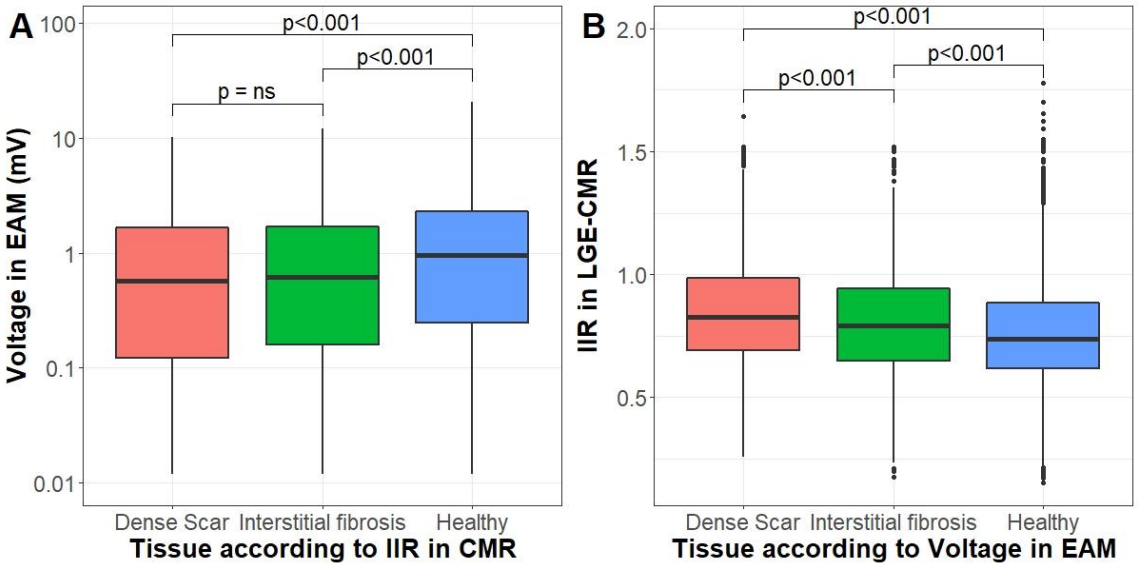

Figure 7. Comparative box plot charts (median and interquartile range values). A: bipolar voltage (EAM) in areas classified as healthy tissue, interstitial fibrosis, and dense scar by IIR (CMR). B: IIR values (CMR) in areas classified as healthy tissue, interstitial fibrosis, and dense scar by EAM. CMR, cardiac magnetic resonance; EAM, electro-anatomical map; IIR, image intensity ratio.

SUPPLEMENTARY DATA

Quantification of right atrial fibrosis by cardiac magnetic resonance: verification of the method to standardize thresholds.

Clara Gunturiz-Beltrán (MD)[a,b,c], Roger Borràs (MSc)[a,b,d], Francisco Alarcón (MSc)[a,b], Paz Garre (MSc)[a,b], Rosa M Figueras I Ventura (MSc, PhD)[e], Eva M Benito (MD)[a,b], Gala Caixal (MD)[a,b], Till F Althoff (MD, PhD)[a,f,g], Jose María Tolosana (MD, PhD)[a,b], Elena Arbelo (MD, PhD)[a,b], Ivo Roca (MD, PhD)[a,b], Susanna Prat-Gonzalez (MD, PhD)[a,b], Rosario Jesus Perea (MD, PhD)[a,b], Josep Brugada (MD, PhD)[a,b], Marta Sitges (MD, PhD)[a,b], Eduard Guasch (MD, PhD)[a,b,c], Lluís Mont (MD, PhD)[a,b,c]

a.Institut Clínic Cardiovascular, Hospital Clínic, Universitat de Barcelona, Catalonia, Spain.

b.Institut d´Investigacions Biomédiques August Pi i Sunyer (IDIBAPS), Barcelona, Catalonia, Spain.

c.Centro de Investigación Biomédica en Red de Enfermedades Cardiovasculares (CIBERCV), Madrid, Spain.

d.Centro de Investigación Biomédica en Red de Salud Mental (CIBERSAM), Instituto de Salud Carlos III, Madrid, Spain.

e.ADAS3D Medical S.L., Barcelona, Catalonia, Spain

f.Department of Cardiology and Angiology, Charité-University Medicine Berlin, Charité Campus Mitte, Berlin, Germany

g.DZHK (German Centre for Cardiovascular Research), Partner Site Berlin, Berlin, Germany

Supplementary Methods:

Cohorts under study

A total of 53 individuals in whom an LGE-CMR had been performed for research purposes were included in consecutive stages of this study. Initially, thresholds to identify fibrosis in the RA were determined in healthy volunteers (18 to 30-year-old individuals without any relevant comorbidity, who had been recruited to assess LA fibrosis threshold,[1] n=9) and patients who had undergone typical atrial flutter and AF ablation in the same procedure (n=9). Later, patients with paroxysmal (n=10) or persistent (n=10) AF were used for validation. Finally, correlation between the IIR and EAM in an additional prospective cohort of patients undergoing a first AF ablation procedure was evaluated (n=15). The exclusion criteria were: age less than 18 years, poor quality of LGE-CMR, severe renal failure (glomerular filtration rate < 30 ml/min), known gadolinium allergy, implanted cardiac electronic device, pregnancy or lactation.

LGE-CMR imaging

An LGE-CMR was obtained in all individuals included in the present study. Details of the healthy volunteers have been reported also previously.[1] In the post-ablation group, LGE-CMR was obtained 3 months after the index ablation procedure. In the validation groups (paroxysmal and persistent AF), an LGE-CMR was performed less than 2 weeks before the ablation procedure.

Acquisition protocol: Images were obtained with a 3.0 Tesla CMR (Magnetom Prisma Siemens Healthcare, Germany) and a dedicated 32-channel cardiac coil, as described previously.[1,2] Electrical cardioversion was performed, if necessary, prior to the LGE-CMR to improve image acquisition and quality. LGE-CMR scans were acquired 20 min after an intravenous bolus injection of 0.2 mmol/kg gadobutrol (Gadovist, Bayer Hispania) using a free-breathing 3D navigator and ECG-gated inversion-recovery gradient-echo sequence applied in the axial orientation. The gadolinium dose was selected for consistency with previous research from our and other groups, and

according to current recommendations.[3] The voxel size was 1.25x1.25x2.5 mm. Repetition time/echo time was 2.3/1.4 ms; flip angle, 11º; bandwidth, 460 Hz/pixel; inversion time (TI) 280 to 380 ms; and parallel imaging with GRAPPA technique, with reference lines of R=2 and 72. A TI scout sequence was used to nullify the left ventricular myocardial signal and determine optimal TI. Typical scan time for a LGE-CMR sequence was 15 minutes (11-18), depending on heart rate and breathing patterns.

Post-processing: Both the RA and LA of each patient were initially segmented by an expert investigator and reviewed by a second expert investigator to ensure optimum image processing. RA and LA segmentation was performed using ADAS 3D software (Barcelona, Spain). Atrial contours of the wall were manually drawn by two expert operators in each axial plane of the LGE-CMR, without invading the interatrial common septum, and a tridimensional model was constructed. ADAS automatically builds a 3D shell. Subsequently, pulmonary veins at the ostium level, mitral valve plane and left appendage were excluded in the LA, and the superior and inferior vena cava at the ostium level, tricuspid valve plane and coronary sinus were excluded in the RA.

Signal intensity was internally (within each patient) normalized to blood pool intensity to provide an absolute signal intensity value that would allow comparisons between patients. The LA blood pool was automatically identified by the software. Image Intensity Ratio (IIR) was calculated as the ratio between the signal intensity of each single pixel and the mean blood pool intensity for each patient. IIR values were colour-coded, projected into the atrial shell, and presented in histograms.

Assessment of total fibrosis and dense scar thresholds

Signal intensity was obtained from each pixel of the RA wall and normalized to the mean LA blood intensity to calculate the image intensity ratio (IIR); an analogous process in the LA wall was performed as a reference. The LA blood pool intensity was

chosen for RA wall normalization because it was found to be less variable than the RA blood pool, and due to enabling comparison between both atria. Notably, the correlation between LA- and RA-blood pool adjusted IIR was very high (r=0.95, Supplementary figure). All the IIR values of each subgroup were represented in histograms, and thresholds calculated as follows. Using a common definition of normality (i.e., mean±2 standard deviations [SD] of a normal cohort),[1] the fibrosis threshold was defined as the mean IIR value in the healthy volunteer group plus 2 SD. By definition≈97.5% of all pixels in the healthy volunteers group fell below this threshold. The dense scar threshold was defined using previously clinically validated algorithms for identifying gaps in LA after PV isolation[4] and ventricular scar heterogeneity[5], as the IIR value corresponding to 60% of the maximum normalized signal intensity pixel in the RA of patients who had undergone cavotricuspid isthmus ablation.

We established an upper limit of healthy tissue IIR in the RA and a threshold discriminating interstitial fibrosis from dense scar. For validation purposes, both values were then used to quantify total, interstitial fibrosis and dense scar in all participants and groups.

Correlation between LGE-CMR and electro-anatomical map

In 15 consecutive patients undergoing AF ablation (8 paroxysmal / 7 persistent), an intraprocedural high density point-by-point electro-anatomical bipolar voltage maps (EAM) of the RA and LA (CARTO 3, Biosense-Webster) were obtained with a multipolar catheter (Lasso, Biosense Webster or Pentarray, Biosense Webster) before ablation. Standard voltage thresholds of 0.1 mV and 0.5 mV were used to characterize the atrial tissue, as follows: dense scar <0.1mV; 0.1mV < interstitial fibrosis < 0.5mV; 0.5mV < healthy tissue.[6]

The EAM was merged with the previously built RA/LA LGE-CMR 3D shell. Both structures were aligned, and only EAM points projected on the CMR 3D image less

than 10 mm apart were used. The correlation between bipolar voltage (in the EAM) and normalized IIR (in the LGE-CMR) values was calculated for each patient. The accuracy of LGE-CMR and the EAM in classifying areas as healthy tissue, interstitial fibrosis or dense scar was also calculated.

Statistical analysis

Continuous variables are shown as mean±SD or median (interquartile range) except if otherwise stated, and comparisons amongst groups were performed with one-way ANOVA. Categorical variables are summarized as total number and percentages. The skewness and kurtosis were computed to characterize the IIR histograms for each group. The Lin concordance correlation coefficient was used to test interobserver agreement. The correlation between IIR and EAM was assessed using the Pearson correlation coefficient (r), and a generalized linear mixed model with random intercept accounted for repeated IIR measurements per patient. The strength of association was evaluated according to the following criteria: weak ≤ 0.3; 0.3 > moderate ≥ 0.7; good > 0.7. Since bipolar voltage was not normally distributed, its log-transformation was used. Overall agreement was calculated as the ratio between the number of pixels in which EAM and MRI yielded the same classification (ie., healthy tissue, dense scar, interstitial fibrosis), and the overall number of pixels. A two-sided type I error of 5% was used for all tests. Because the study was not designed to be a hypothesis testing study involving a null and alternative hypothesis, a sample size was estimated using similar number of participants than in previous work in the field.[1,7] For IIR histogram, but also correlation, analyses were performed in several thousand of data points. All analyses were performed using R v3.5.1 (R project for Statistical Computing).

REFERENCES:

1. Benito EM, Carlosena-Remirez A, Guasch E, et al. Left atrial fibrosis quantification by late gadolinium-enhanced magnetic resonance: a new method to standardize the thresholds for reproducibility. *Europace*. 2017;19(8):1272-1279.
2. den Uijl DW, Cabanelas N, Benito EM, et al. Impact of left atrial volume, sphericity, and fibrosis on the outcome of catheter ablation for atrial fibrillation. *J Cardiovasc Electrophysiol*. 2018;29(5):740-746.
3. Kramer CM, Barkhausen J, Bucciarelli-Ducci C, Flamm SD, Kim RJ, Nagel E. Standardized cardiovascular magnetic resonance imaging (CMR) protocols: 2020 update. *J Cardiovasc Magn Reson*. 2020;22(1):1-18.
4. Bisbal F, Guiu E, Cabanas-Grandío P, et al. CMR-guided approach to localize and ablate gaps in repeat AF ablation procedure. *JACC Cardiovasc Imaging*. 2014;7(7):653-663.
5. Andreu D, Berruezo A, Ortiz-Pérez JT, et al. Integration of 3D electroanatomic maps and magnetic resonance scar characterization into the navigation system to guide ventricular tachycardia ablation. *Circ Arrhythm Electrophysiol*. 2011;4(5):674-683.
6. Khurram IM, Beinart R, Zipunnikov V, et al. Magnetic resonance image intensity ratio, a normalized measure to enable interpatient comparability of left atrial fibrosis. *Heart Rhythm*. 2014;11(1):85-92.
7. Bertelsen L, Alarcón F, Andreasen L, et al. Verification of threshold for image intensity ratio analyses of late gadolinium enhancement magnetic resonance imaging of left atrial fibrosis in 1.5T scans. *Int J Cardiovasc Imaging*. 2020;36(3):513-520.

Supplementary figure

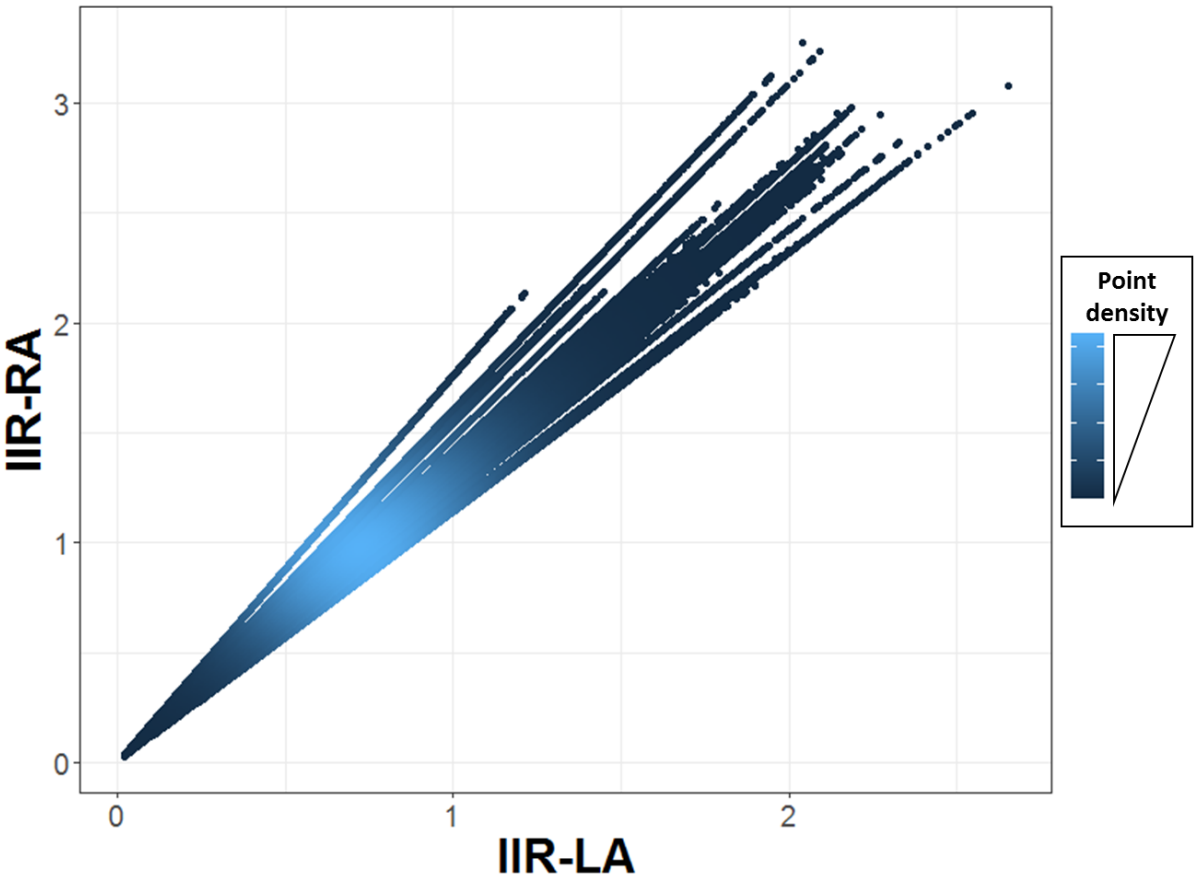

Correlation between left atrium (LA) blood pool- and right atrium (RA) blood pool-standardized image intensity ratio. Correlation, estimated by the Pearson correlation coefficient was found to be very high (r=0.95).